ACS OMEGA

Open Access

http://pubs.acs.org/journal/acsodf

Article

Valorization of Rejected Macroalgae *Kappaphycopsis cottonii* for Bio-Oil and Bio-Char Production via Slow Pyrolysis

Obie Farobie,* Apip Amrullah, Novi Syaftika, Asep Bayu, Edy Hartulistiyoso, Widya Fatriasari, and Asep Bayu Dani Nandiyanto

Cite This: *ACS Omega* 2024, 9, 16665−16675

Read Online

ACCESS | Metrics & More | Article Recommendations | Supporting Information

ABSTRACT: *Kappaphycopsis cottonii*, a prominent macroalgae species cultivated in an Indonesian marine culture, yields significant biomass, a portion of which is often rejected by industry. This study explores the potential valorization of rejected *K. cottonii* biomass through slow pyrolysis for bio-oil and biochar production, presenting an alternative and sustainable utilization pathway. The study utilizes a batch reactor setup for the thermal decomposition of *K. cottonii*, conducted at temperatures between 400 and 600 °C and varying time intervals between 10 and 50 min. The study elucidates the temperature-dependent behavior of *K. cottonii* during slow pyrolysis, emphasizing its impact on product distributions. The results suggest that there is a rise in bio-oil production when the pyrolysis temperature is raised from 400 to 500 °C. This uptick is believed to be due to improved dehydration and greater thermal breakdown of the algal biomass. Conversely, at 600 °C, bio-oil yield diminishes, indicating secondary cracking of liquid products and the generation of noncondensable gases. Chemical analysis of bio-oils reveals substantial quantities of furan derivatives, aliphatic hydrocarbons, and carboxylic acids. Biochar exhibits calorific values within the range of 17.52−19.46 MJ kg^{-1}, and slow pyrolysis enhances its specific surface area, accompanied by the observation of carbon nanostructures. The study not only investigates product yields but also deduces plausible reaction routes for the generation of certain substances throughout the process of slow pyrolysis. Overall, the slow pyrolysis of rejected *K. cottonii* presents an opportunity to obtain valuable chemicals and biochar. These products hold promise for applications such as biofuels and diverse uses in wastewater treatment, catalysis, and adsorption, contributing to both environmental mitigation and the circular economy.

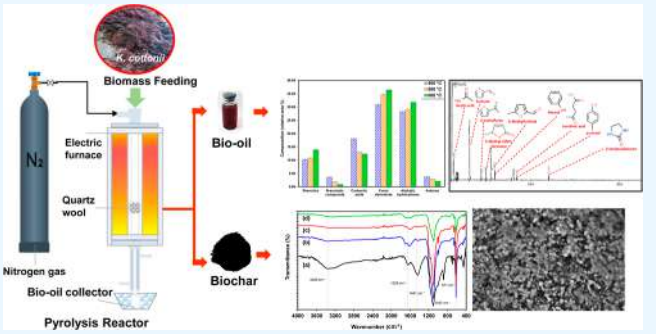

1. INTRODUCTION

In response to escalating global energy demands and climate change concerns, exploring sustainable alternatives to fossil fuels is imperative. Biomass is widely acknowledged as a green substitute for conventional energy and carbon supply, providing a renewable and sustainable solution.[1] Various methods have emerged to harness biomass energy, encompassing biochemical and thermochemical conversion processes. Although biochemical conversion exhibits lower energy intensity compared to thermochemical processes, its economic feasibility is hindered by limitations. In contrast, thermochemical biomass conversion involving methods like torrefaction,[2,3] gasification,[4−6] and pyrolysis[7−9] is favored due to its efficiency and cost-effectiveness.[10] Among various thermochemical conversion methods, pyrolysis is particularly notable for its widespread use in transforming biomass into useful chemicals and biofuels. This prominence is attributed to the process's energy-efficient and cost-effective characteristics.[11] In particular, slow pyrolysis, characterized by its controlled heating rates and extended residence times, offers several advantages.[12] It facilitates the preservation of biomass components, resulting in higher quality bio-oil and biochar products. The slow heating process also minimizes the formation of undesired byproducts, enhancing the overall efficiency of biomass conversion.[13]

Recent studies have extensively explored the production of bio-oil and biochar from various biomass sources through pyrolysis.[14,15] Concerns about food versus fuel competition in using first-generation biofuel sources have prompted the exploration of third-generation biomass options like macroalgae. Macroalgae offer numerous benefits, such as increased biomass yields and accelerated growth rates, contrasting with those observed in land-based plants.[16] Additionally, they can thrive in various water sources, including seawater, freshwater, and wastewater, without the need for arable land and

Received: January 20, 2024
Revised: March 14, 2024
Accepted: March 15, 2024
Published: March 28, 2024

fertilizers.[17] *Kappaphycopsis cottonii*, also known as *Kappaphycus alvarezii* or *Eucheuma cottonii*, is a widely cultivated macroalgae in Indonesian marine culture. However, while it yields significant biomass, a considerable portion is often rejected because its carrageenan content is only 25−35%.[18] A significant portion of seaweed solid waste goes unused, with the majority being discarded as waste, thereby contributing to environmental pollution.[19] These organic constituents remain viable for conversion into valuable products.

Harnessing the valuable products of this rejected biomass becomes not only an environmental necessity but also a strategic move toward a more sustainable and circular economy. Given its tremendous potential, rejected *K. cottonii* from industries can be processed through pyrolysis to produce bio-oil and biochar. Nevertheless, there is a scarcity of studies and applications related to the utilization of *K. cottonii*, especially its waste from the carrageenan industries. A previous study employed pyrolysis within 300 to 600 °C for a duration of 1 h to treat various macroalgae species, including *Undaria pinnatifida*, *Laminaria japonica*, and *Porphyra tenera*. However, this investigation did not use *K. cottonii* and concentrated solely on the bio-oil products, providing no detail on the biochar. Recent studies by our group previously explored the degradation rate of slow pyrolysis using different species, named *Sargassum plagiophyllum* and *Ulva lactuca*, to obtain bio-oil and biochar.[13,20] A study conducted by Saeed et al.[21] utilized *E. cottonii* as feedstock, employing pyrolysis with a tube furnace with N_2 gas at temperatures of 250 and 550 °C for 120 min. However, this study focused only on biochar production for environmental applications, specifically to absorb methylene blue dye, without exploring the bio-oil product.

The previously mentioned study has suggested the possible application of *K. cottonii* macroalgae in pyrolysis to generate fuels and chemicals. Nevertheless, there remains a gap in understanding the specific effects of different pyrolysis residence times and temperatures on the product properties. This study, therefore, seeks to fill this gap by conducting a thorough investigation into the behavior of *K. cottonii* during slow pyrolysis. The focus of this study is to elucidate the effects of different pyrolysis residence times at different temperatures on the product properties. Understanding how varying pyrolysis conditions impact the quality and yield of bio-oil and biochar is crucial for optimizing the process and maximizing its potential. Furthermore, the study aims to clarify the plausible reaction pathways involved in the pyrolysis of *K. cottonii*. By offering insights into these reaction pathways, a better understanding of the decomposition process of *K. cottonii* through pyrolysis can be achieved. Consequently, the in-depth examination of *K. cottonii* valorization via pyrolysis stands to contribute not only to environmental mitigation and bioenergy production but also to providing valuable information for the development of value-added chemicals. This research can pave the way for more nuanced exploration and implementation in future studies.

2. MATERIALS AND METHODS

2.1. Preparation and Analysis of Feedstock. The residual matter of *K. cottonii* macroalgae was sourced from the waste products of a local carrageenan manufacturing facility, PT. Bantimurung, in South Sulawesi. Initially, the macroalgae rejections underwent a thorough rinse to remove foreign materials and were then left to air-dry. Following this, the samples were kept in a cold storage environment at about 3.5 °C, surrounded by Styrofoam insulation for temperature control, and shipped to IPB University in Bogor, Indonesia. At the university, the macroalgae were subjected to heat dehydration in an oven set at 105 °C for a duration of 12 h. Following this, the macroalgal feedstock was then pulverized and sifted to attain a consistent size of 0.25 mm.

The algal material was subjected to proximate composition analysis using a PerkinElmer thermogravimetric analyzer following the guidelines outlined in ASTM E1131-08. The weight reduction after heating at 110 °C in a nitrogen atmosphere was measured as the moisture content. Meanwhile, the weight loss at a temperature of 900 °C was determined to be that of volatile matter. The residue left after the sample was maintained for 45 min was regarded as the ash quantity. By subtracting the weight percentages of the volatile components, moisture, and ash from 100, the fixed carbon content was determined (eq 1).

$$\text{FC (wt \%)} = 100 - (\text{volatile matter wt \%} + \text{moisture wt \%} + \text{ash wt \%}) \quad (1)$$

The investigations into the levels of carbohydrates, fats, and proteins were conducted at PT. Saraswanti Indo Genetech, a certified laboratory under ISO/IEC 17025. An automatic Kjeldahl apparatus (Kjeltec 8400 by Foss, Denmark) was employed for protein estimation. The higher heating values (HHVs) of the macroalgal feedstock were calculated using a Parr 6200 bomb calorimeter. The calculations were carried out according to the standard method, ASTM D 5865-04. The CHN628 and CHN632 elemental analyzers from Leco were employed to conduct elemental analysis. The oxygen percentage was deduced by the formula shown in the following equation

$$\text{oxygen (\%)} = 100 - (\%\,\text{C} + \%\,\text{H} + \%\,\text{N} + \%\,\text{S}) \quad (2)$$

To ensure the reliability and accuracy of the results, all analyses were conducted in triplicate.

2.2. Pyrolysis of Red Macroalgae *K. cottonii*. The process of pyrolyzing the *K. cottonii* red macroalgae was conducted in a sealed stainless-steel reactor, as depicted in Figure 1. The equipment included a heating furnace, a

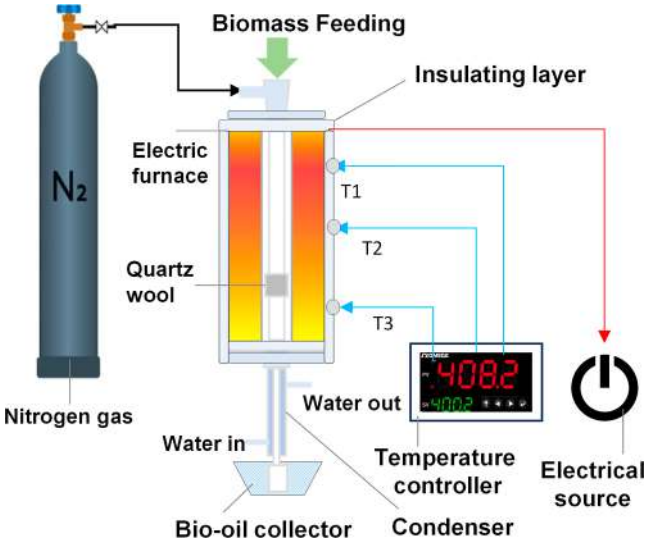

Figure 1. Schematic diagram of the experimental apparatus.

https://doi.org/10.1021/acsomega.4c00678
ACS Omega 2024, 9, 16665−16675

temperature measurement device (thermocouple), and a cooling system. The design of the reactor was such that it could handle temperatures as high as 1000 °C, with a proportional integral derivative controller managing the temperature regulation. A 50 g portion of the dehydrated algae was placed into the reactor to undergo pyrolysis. Subsequently, nitrogen gas was flowed into the reactor at a rate of 50 mL min^{-1} to eliminate the presence of air. The macroalgal biomass was gradually heated from ambient temperature to specific target temperatures (400, 500, and 600 °C), with a heating rate of 50 °C per minute. Each temperature level was maintained for duration intervals of 10, 30, and 50 min for the pyrolysis reactions. The gases generated from pyrolysis were condensed into a liquid state and collected at a designated sampling port. Any liquid byproducts remaining in the reactor were dissolved with dichloromethane. Anhydrous sodium sulfate was then used to extract water from the liquid byproduct. The process further involved the separation of the liquid phase from the solid content through vacuum filtration. A rotary evaporator was subsequently employed to separate the soluble content from the collected bio-oil. The bio-oil's weight was measured for yield determination, while the solid residue, biochar, was also weighed using gravimetry. To ensure consistency in the results, all of the experimental trials were replicated three times. Relevant calculation formulas were employed to determine the product yields, as previously reported in our earlier publication.[13]

2.3. Product Characterization. The analysis of the bio-oil fraction involved the utilization of a gas chromatography/mass spectrometry (GC/MS) instrument, which was equipped with an Rtx-5MS capillary column (15 m length × 0.25 mm inner diameter × 0.10 μm in thickness). A column flow rate of 2 mL min^{-1} and a split ratio of 10:1 were used. This analysis employed helium as the carrier gas. Prior to injection into the GC/MS system, the bio-oil was diluted with dichloromethane using a volumetric ratio of 1 to 4. The thermal protocol for the analysis started with the oven set at 40 °C for 1 min. Afterward, the temperature was escalated at 10 °C/min to reach 150 °C, where it remained for 5 min. Following this, the temperature was further ramped to 300 °C at 10 °C/min and was maintained at that level for half an hour. The ion source in the mass spectrometer utilized an electron ionization potential of 70 eV, while the detector temperature was kept at 250 °C. The compounds separated from the bio-oil vapors underwent scanning within a mass-to-charge (m/z) range of 35−700 Da. Identification of these compounds was achieved by matching their mass spectra with those available in the NIST2008 c2.0/Xcalibur database. Compounds exhibiting response factors greater than 85% were included in the subsequent analysis, with their abundance expressed as a percentage of the relative peak area. This relative peak area percentage may also correspond to the selectivity percentage of the compounds. An aliquot of 1 μL of the sample was injected for the assessment.

For the solid biochar residues resulting from *K. cottonii* pyrolysis, several characterization techniques were employed. Their fundamental elemental analysis (C, H, N, and S) was evaluated using techniques identical to those applied to the original feedstock. Fourier transform infrared spectroscopy (FTIR) analysis was conducted to determine the functional groups present in the sample using a PerkinElmer spectrometer. The biochar samples were evenly distributed across the diamond crystal, ensuring that the crystal was fully coated with the sample. The spectrometer settings were adjusted to scan wavelengths from 400 to 4000 cm^{-1} with a resolution of 4 cm^{-1}, compiling a total of 16 scans. The structural morphology of biochar was investigated under a scanning electron microscope (model: Hitachi SU 3500). A simultaneous SEM−EDX (energy-dispersive X-ray) setup was utilized to analyze the elemental composition further. Lastly, the pore structure and surface area were quantitatively measured using a Brunauer−Emmett−Teller (BET) analyzer from Anton Paar, specifically the Quantachrome Nova series. The method of BET nitrogen gas physisorption was utilized at 77 K across a relative pressure span of $P/P0 = 0.01−0.99$. Prior to conducting the N_2 adsorption tests, the biochar specimens underwent degassing in the analyzer for 3 h at 120 °C. The collected data from N_2 adsorption were then analyzed to calculate the BET-N_2 surface area and the total pore volume. Moreover, the elemental composition of biochar, specifically carbon (C), hydrogen (H), and nitrogen (N), was assessed using a CHN628 analyzer (Leco), while the sulfur (S) content was analyzed with a CHN632 analyzer (Leco). Each experiment utilized a sample mass of approximately 0.15 g. An elemental analyzer typically features a combustion tube within a dual-stage furnace heated to approximately 1000 °C in the presence of pure oxygen. This arrangement ensures the thorough combustion of organic specimens, negating the need for extra metal oxidizing agents or distinct carrier gases. During combustion, the elements—carbon, hydrogen, nitrogen, and sulfur—are transformed into their oxide forms. A carrier gas then delivers the combustion gases to separate infrared cells for measuring H_2O and CO_2 levels and a thermal conductivity cell for nitrogen detection. The oxygen (O) content was deduced using the equation, O (%) = 100 − (% C + % H + % N + % S). To ensure data reproducibility, all analyses were performed at least three times.

3. RESULTS AND DISCUSSION

3.1. Characteristics of Rejected *K. cottonii*. Initially, the chemical, proximate, and elemental compositions of the unprocessed *K. cottonii* were evaluated. It is important to recognize that this analysis was applied to *K. cottonii* that was dried under solar conditions. The findings from the analyses of the sun-dried *K. cottonii* can be seen in Table 1. It is worth noting that the data presented in the tables with ± values represent the mean ± standard deviation of the measurements. The data reveal that the sun-dried *K. cottonii* exhibits a moisture level of approximately 8.33 ± 0.04 wt %. This moisture level is consistent with that found in a similar species from Sabah, Malaysia, which had a recorded moisture content of 7.32%.[21] In contrast, a study by Jumaidin et al.[19] reported a significantly lower moisture content of 1.13% in *K. cottonii* from the eastern coast of Sabah, Malaysia. Additionally, a study by Saldarriaga-Hernandez et al.[22] brought attention to the significant variation in moisture content observed in macroalgae. This variability is affected by several factors, including the specific type of algae, seasonal variations, predrying methods, and the geographic location of harvesting.

Moreover, *K. cottonii* exhibits a notably high ash percentage at 23.28 ± 0.02 wt %, which is substantially greater than more conventional lignocellulosic sources, such as coconut shells, documented at 1.05 wt % ash content.[23] The findings from the SEM−EDX detailed in Figure 2 indicate that potassium (K) predominates as the principal macronutrient within *K. cottonii*,

https://doi.org/10.1021/acsomega.4c00678
ACS Omega 2024, 9, 16665−16675

Table 1. Proximate, Chemical Composition, and Ultimate Analysis of Dried *K. cottonii*

parameters	value
Proximate Analysis (wt %)	
moisture	8.33 ± 0.04
ash content[a]	23.28 ± 0.02
fixed carbon[a]	10.01 ± 0.06
volatile matter	58.38 ± 0.18
Chemical Constituent (wt %)	
carbohydrates	61.90 ± 0.12
proteins	4.77 ± 0.08
lipids	1.72 ± 0.04
others[b]	31.61
Ultimate Analysis (wt %)	
C	30.00 ± 0.25
H	5.27 ± 0.02
N	1.21 ± 0.01
S	9.34 ± 0.12
O[c]	54.18 ± 0.45
HHV (MJ kg^{-1})	10.96 ± 0.03

[a]Dry base. [b]Calculated by the difference. [c]O = 100% − C − H − N − S − ash.

with sodium (Na) and magnesium (Mg) also present in considerable quantities. Research by Kaewpanha et al.[24] has shown that the presence of group 1 and group 2 metals, like potassium and calcium, fulfills a critical function in promoting the degradation of carbon-based materials, facilitating tar breakdown, and aiding in the transformation of char into gaseous products during pyrolysis and gasification processes. Furthermore, Li et al.[25] observed that the presence of inorganic materials in biomass facilitated additional cracking of volatile compounds, leading to gas formation.

With regard to its chemical profile, *K. cottonii* is rich in carbohydrates, constituting 61.90 ± 0.12 wt %, which are predominantly present as polysaccharides and sugar monomers in algae, like carrageenan and agar, particularly in red macroalgae varieties.[26] These carbohydrates have the potential to transform into furanic compounds during pyrolysis.[27] The protein percentage in *K. cottonii*, as determined in the present study, was relatively low, measuring 4.77 ± 0.08 wt % of the dry mass. This figure aligns closely with the protein level in *K. cottonii* from the coastal region of Ramanathapuram district, India, which stood at around 4.5 wt %.[28] Furthermore, Nallasivam et al.[29] have reported a slightly higher protein content of 6 ± 0.2 wt % in *E. denticulatum* from India.[29] The protein levels in marine macroalgae are subject to variation, influenced by species-specific factors and environmental conditions such as location, seasonal changes, and harvest timing.[30] During pyrolysis, the proteins present can play a significant role in the production of bio-oil enriched with nitrogen.[31]

3.2. Influence of Temperature on Product Fraction.

To investigate the influence of different temperatures and dwell times on pyrolysis product ratios of *K. cottonii*, experiments were carried out within a 400−600 °C thermal scope. Throughout the observation, a notable pattern emerged, indicating a significant reduction in the proportion of biochar as the temperature intensified from 400 to 600 °C, as depicted in Figure 3. This decline in biochar content can be primarily attributed to the heightened primary degradation of the macroalgae material when exposed to higher temperatures.[32] Notably, the bio-oil fraction initially experiences a surge between 400 and 500 °C. This rise has been linked to the intensified occurrence of primary degradation reactions such as dehydration and thermal cracking within the algae. Nonetheless, this bio-oil fraction was found to diminish upon exceeding 600 °C because of additional cracking processes that produced an elevated amount of noncondensable gases, including CH_4, CO, and CO_2—confirmed by the noticeably elevated gas product yields at higher temperatures.[32]

At the starting temperature, i.e., 400 °C, the yield of bio-oil was on the lower side, registering just 12.05% after a pyrolysis duration of 10 min, an indication of *K. cottonii* pyrolysis not reaching completion. When the reaction time was extended to 30 and 50 min, the bio-oil yields rose to approximately 17.49 and 21.38%, respectively, owing to the enhanced occurrence of thermal breakdown and moisture removal, thereby augmenting the yield of liquid products. In parallel, biochar yields showed a considerable decrease over time, underlining the extended breakdown of the macroalgae due to the pyrolysis of heftier hydrocarbon chains at extended durations. Comparatively, it was observed that the algal biomass had a more effective conversion to bio-oil at 500 °C. The yields of bio-oil after 10, 30, and 50 min of pyrolysis were approximately 16.32, 22.95, and 28.51%, respectively. It was observed that at a heightened temperature of 600 °C, extending the pyrolysis duration did not significantly enhance the yield of bio-oil.

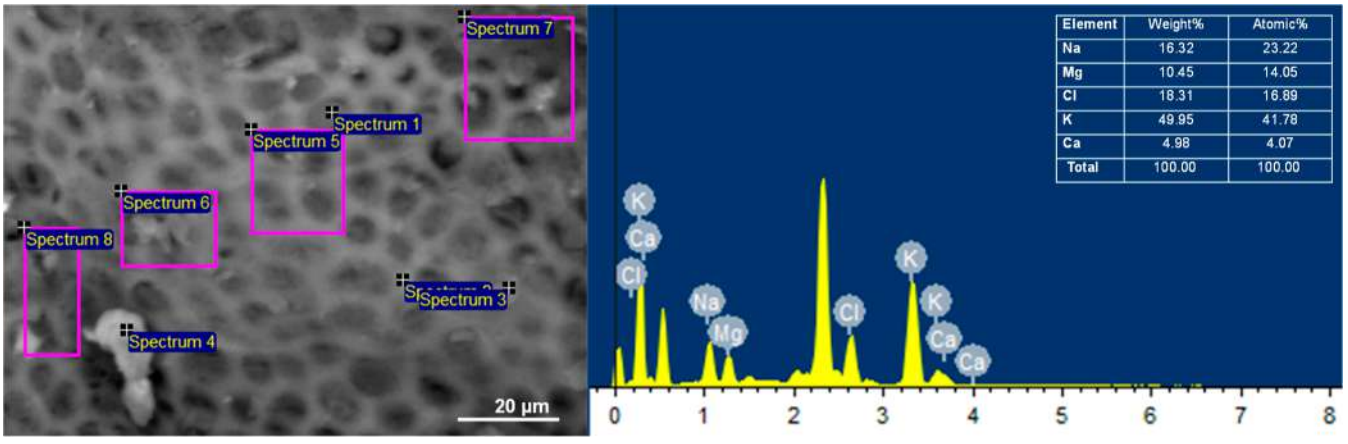

Figure 2. SEM−EDX analysis of dried *K. cottonii*.

https://doi.org/10.1021/acsomega.4c00678
ACS Omega 2024, 9, 16665−16675

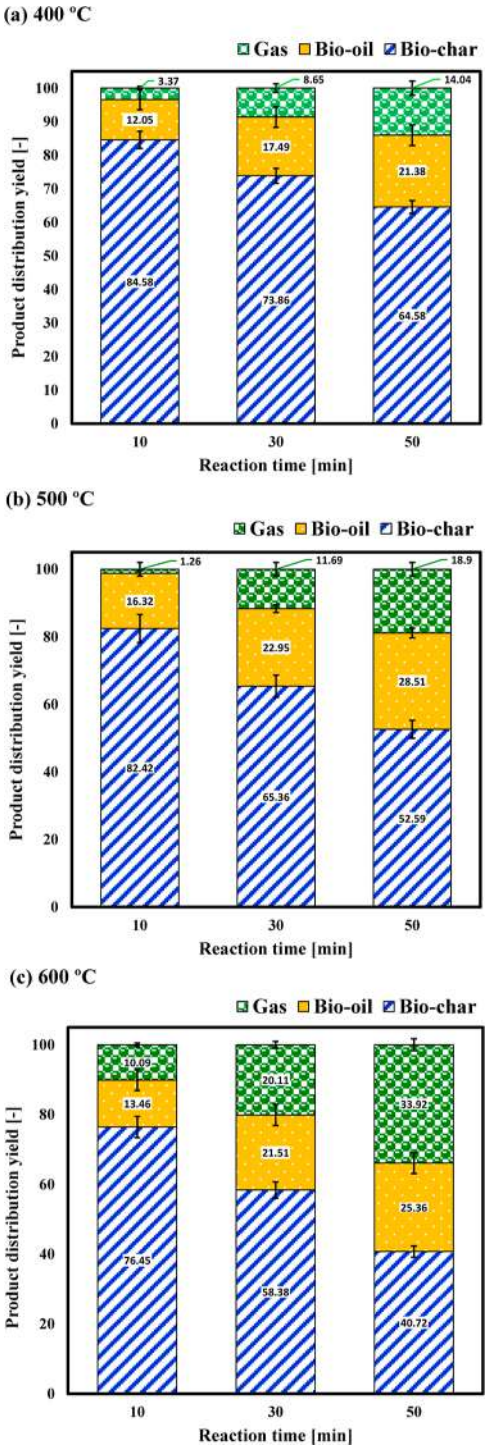

Figure 3. Effect of temperature and reaction time on product distributions of *K. cottonii* pyrolysis at (a) 400, (b) 500, and (c) 600 °C.

All in all, an upward shift in the temperature from 400 to 600 °C corresponded with a swifter decline in biochar yield and an elevation in gaseous products because of the advanced breakdown of both the biochar and pyrolysis vapors. Conversely, the yield of bio-oil reached its pinnacle at a temperature of 500 °C, resonating with outcomes from prior research.[32,33] Works by Zhou et al. on the slow pyrolysis within a 400−600 °C range revealed a decisive fall in biochar from 47.5−51.0% at 400 °C to 40.2−44.8% at 600 °C, while gas yields escalated from 15.8 to 24.7%.[33] Furthermore, in a similar vein, Aboulkas et al.[32] observed a consistent pattern in the pyrolysis of algal waste. They observed a gradual rise in the yield of gaseous products, increasing from 21.81 to 31.44 wt % when the temperature was raised from 400 to 600 °C. In contrast, the quantity of biochar experienced a noticeable decline, decreasing markedly from 52.09 to 40.36 wt %.

Apart from that, it is interesting to note that gas production at 500 °C for 10 min is lower than that at 400 °C. This unexpected result is primarily due to the quicker breakdown of algae into bio-oil, known as primary decomposition, overshadowing the conversion of volatile compounds into gas, or secondary cracking, within this short time. Normally, higher temperatures would boost gas production by promoting the breakdown of these compounds. However, with only 10 min at 500 °C, there is not enough time for secondary cracking to surpass the effects of primary decomposition. This is evident from the increase in bio-oil yield to 16.32% at 500 °C, up from 12.05% at 400 °C, underscoring the limited opportunity for secondary reactions to significantly influence the outcome within such a short time frame.

Consistent with this study's subsequent findings, a considerable biochar yield of around 52.59% can be realized at 500 °C within a period of 50 min. Therefore, subsequent characterizations of biochar properties were concentrated on samples obtained from a 50 min pyrolysis period.

3.3. Bio-Oil Composition. The GC/MS analysis revealed that the bio-oil obtained from *K. cottonii* pyrolysis encompassed a range of different substances, and the area percentages of detected peaks were used to gauge compound abundance based on corresponding response factors. This analysis revealed a complex assortment of bio-oil constituents predominantly made up of furan derivatives, organic acids, aliphatic hydrocarbons, phenolics, ketones, and *N*-heteroaromatics, as depicted in Figures S1−S3.

In assessing the influence of temperature on the composition of bio-oil, the study focused on major compounds exhibiting an area percentage greater than 0.5%. Table S1 presents the varying quantities of these compounds at different pyrolysis temperatures. At 400 °C, GC/MS analysis identified the most prolific compounds as propane (28.24%), furfural (19.88%), and acetic acid (18.11%). The generation of propane is typically due to the decomposition of organic acids and decarboxylation.[1] Furfural's emergence results primarily from the decomposition of cellulose,[34] with a distinct increase in yield from 19.88 to 21.17% as the temperature rose from 400 to 500 °C, suggesting that temperatures exceeding 400 °C favor the cellulose dehydration process that produces furfural.[27] At a higher temperature of 600 °C, significant amounts of phenols appear, likely generated from reactions involving steam and aromatic compounds during biomass pyrolysis.[34]

Figure 4 further stratifies the chemical composition of the *K. cottonii* bio-oil into several categories, such as furan derivatives, aliphatic hydrocarbons, carboxylic acids, phenolic substances, ketones, and nitrogenous aromatics. Predominantly, the bio-oil composition was significantly made up of furan compounds, occupying area percentages between 30.96 and 36.44%. Derivation of furan compounds is typically a product of the thermal decomposition of glucose-derived carbohydrates and marine algae's complex sugars.[27,35] Zhou et al.[36] reported that such furan derivations could result from a sequence of dehydration and ring-opening mechanisms acting upon xylose

https://doi.org/10.1021/acsomega.4c00678
ACS Omega 2024, 9, 16665−16675

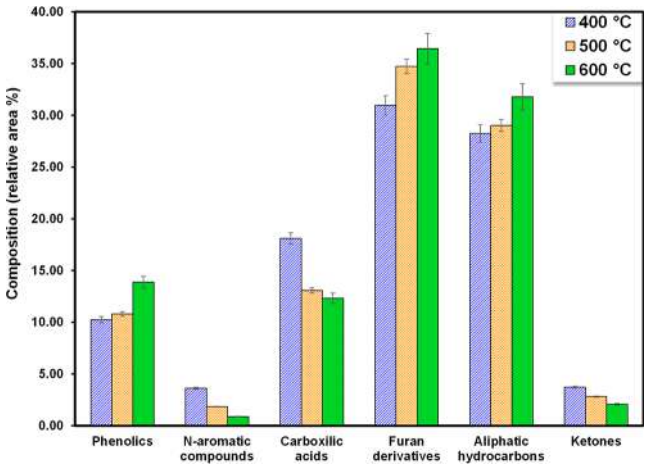

Figure 4. Compounds observed in bio-oil from the pyrolysis of *K. cottonii* at varied temperatures.

molecules. Additionally, these compounds could form via concerted electrocyclic processes accompanied by successive dehydration and cyclization steps. The analysis demonstrated that the bio-oil exhibited an increasing preference for furan compounds when exposed to elevated temperatures, presenting a pattern of increase: 30.96% at 400 °C, 34.73% at 500 °C, and 36.44% at 600 °C. This trend suggests the enhancement of ring-opening and fragmentation of furan compounds, promoting the formation of various hydrocarbons, which proliferate with thermal elevation.

Figure 5 illustrates the plausible chemical transformations occurring during the slow pyrolysis of *K. cottonii*. The bio-oil produced from the thermal degradation of *K. cottonii* was discovered to contain a significant abundance of aliphatic hydrocarbons, with propane being the sole hydrocarbon detected in this fraction. The formation of this hydrocarbon predominantly occurs through a combination of the cracking of organic acids and decarboxylation reactions. With a rise in operational temperatures, a trend of increased concentrations of aliphatic hydrocarbons in the bio-oil was observed, which presented itself in the following sequence: 28.24% at 400 °C, 29.02% at 500 °C, and 31.78% at 600 °C. These aliphatic hydrocarbons are believed to arise from processes such as ring-opening reactions, cracking, and the removal of water from cellulose, akin to the mechanisms described by Iaccarino and colleagues.[1]

Notably, the thermal decomposition of *K. cottonii* resulted in an elevated level of carboxylic acids, ranging from 12.32 to 18.11%, a concentration higher than typically found in terrestrial lignocellulosic biomass.[37−39] This abundance of short-chain carboxylic acids in bio-oil is commonly linked to the breakdown of fatty acid chains. These findings concur with those reported by Iaccarino et al.,[1] who documented a substantial presence of organic acids in the liquid product produced from the halophyte *Salicornia bigelovii*. Moreover, their study revealed that as the pyrolysis temperature increased, the proportion of carboxylic acids in the bio-oil showed a diminishing trend, starting from 18.11% at 400 °C, dropping to 13.07% at 500 °C, and further to 12.32% at 600 °C. This could be attributed to the decarboxylation and temperature degradation occurring within organic acids, leading to the formation of short-chain aliphatic hydrocarbons, which incidentally exhibited an increased trend with rising pyrolysis temperatures.

The bio-oil derived from *K. cottonii* pyrolysis had a comparatively low content of phenolic components. The proportion of these compounds was recorded at 10.24, 10.80, and 13.88% for the respective temperatures of 400, 500, and 600 °C. Such levels are modest when compared to the phenolic yields from the pyrolysis of land-based lignocellulosic materials, where their production is notably higher, ranging

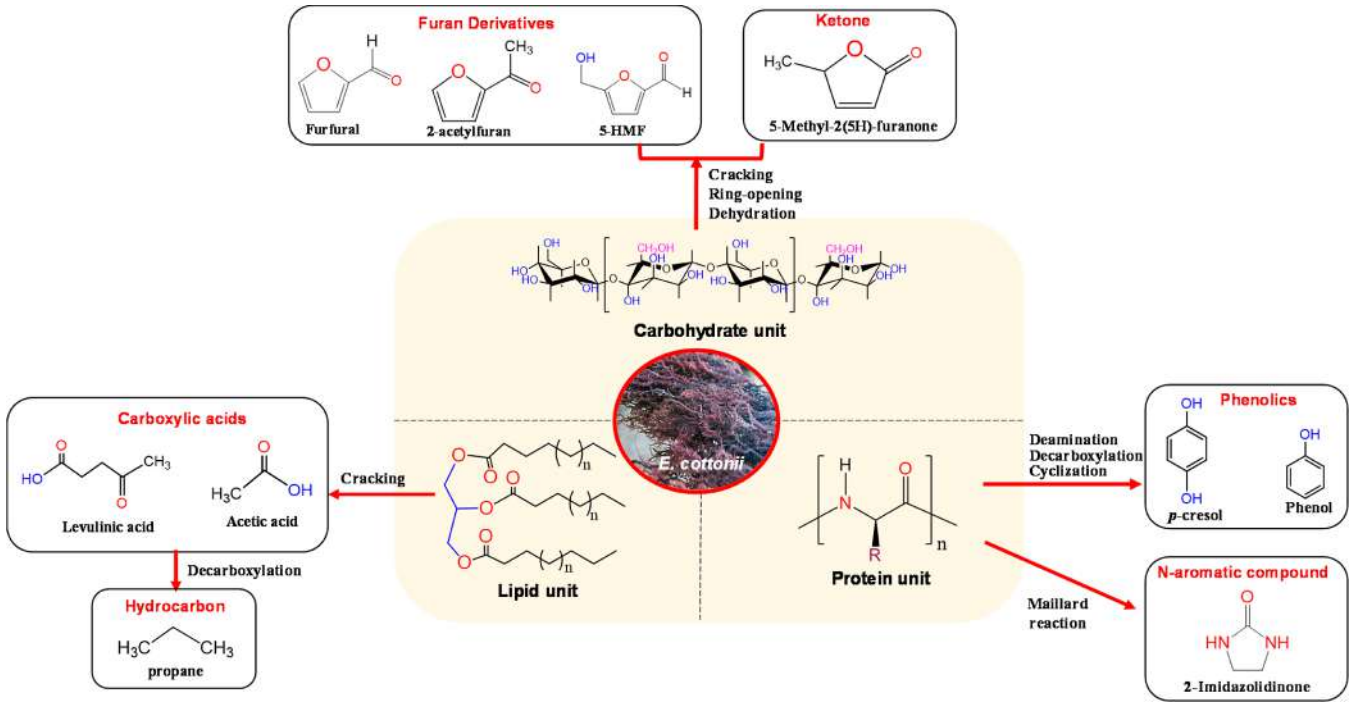

Figure 5. Plausible reaction pathways from slow pyrolysis of *K. cottonii*.

https://doi.org/10.1021/acsomega.4c00678
ACS Omega 2024, 9, 16665−16675

Table 2. Elemental Composition in Biochar Derived from the Pyrolysis of *K. cottonii*

sample	ultimate analysis (wt %, dry ash free)					HHV (MJ/kg)
	% C	% H	% N	% S	% O	
feedstock	30.00 ± 0.25	5.27 ± 0.02	1.21 ± 0.01	9.34 ± 0.12	54.18 ± 0.45	10.96 ± 0.03
biochar (300 °C)	38.90 ± 0.34	3.18 ± 0.02	1.53 ± 0.16	9.06 ± 0.04	47.32 ± 0.48	17.52 ± 0.09
biochar (400 °C)	39.99 ± 0.24	3.13 ± 0.02	1.52 ± 0.40	9.01 ± 0.10	46.35 ± 0.24	18.34 ± 0.07
biochar (500 °C)	40.47 ± 0.07	2.49 ± 0.15	1.30 ± 0.33	8.73 ± 0.03	47.01 ± 0.38	19.46 ± 0.10

from 28.1 to 65.56%.[40,41] The modest phenolic content in the bio-oil derived from *K. cottonii* could be a result of macroalgae generally having a lower lignin concentration than terrestrial vegetation.[16] Additionally, the emergence of phenolic derivatives is often associated with the breakdown of protein structures, particularly those proteins that include the amino acid phenylalanine. Furthermore, the generation of these compounds may be facilitated by the interaction between water and aromatic components in the biomass, as described by Gautam et al.[34]

The bio-oil yielded from *K. cottonii* pyrolysis contained only modest levels of nitrogen-containing aromatic molecules. These *N*-aromatic compounds typically form through the breakdown of proteins into their constituent amino acids when subjected to the high temperatures of pyrolysis, which then undergo further transformations via cyclization and aromatization.[16] An alternative pathway for their formation could involve the Maillard reaction, which occurs when amino acids and carbohydrates react together, leading to the breakdown and subsequent generation of *N*-aromatic structures.[42] This observation aligns with the findings by Iaccarino et al.,[1] where amino acids were shown to undergo transformations such as decarboxylation, cyclization, and dehydration, resulting in the creation of nitrogenous heterocyclic compounds during the pyrolysis of the halophyte *S. bigelovii*. Additionally, it was identified that *K. cottonii* yielded only a small quantity of ketones. This aligns with previous research indicating that ketones are primarily formed through the decomposition of cellulose and hemicellulose.[43,44]

3.4. Characteristics of Biochar. The biochar produced underwent analysis to ascertain its elemental composition, identify its functional groups, and explore its surface characteristics. This was carried out to gain deeper insight into the pyrolytic conversion process of *K. cottonii*.

3.4.1. Elemental Composition. Table 2 presents the energy content and comprehensive elemental analysis of the biochar derived from *K. cottonii*, with the original macroalgal biomass values provided for comparative analysis. The biochar generated exhibited an augmented carbon (C) profile in comparison with the raw feedstock. Additionally, there was an uptick in the carbon content within the biochar as the temperature rose. Conversely, the levels of oxygen (O) and hydrogen (H) in the biochar were found to be reduced relative to the feedstock, potentially due to the occurrence of dehydration as well as decarbonylation and decarboxylation reactions at elevated temperatures.[1]

The proportion of hydrogen in the biochar demonstrated a decreasing pattern with the elevation in temperature, decreasing from 3.18% at 400 °C to 3.13% at 500 °C and further to 2.49% at 600 °C. The potential reason for the decrease in hydrogen and oxygen levels may be that higher temperatures enhance deoxygenation and dehydration reactions. The limited presence of hydrogen in the biochar can also be attributed to the generation of H_2 gas through the aromatization process and the production of low-molecular-weight hydrocarbons such as CH_4 or C_2H_4.[32] Additionally, it is important to note that as the temperature of the pyrolysis process increases, the nitrogen level in the biochar resulting from the pyrolysis of macroalgae decreases. This decrease may be caused by the emission of nitrogen in the gaseous form.

Additionally, it is important to mention that the HHV of the biochar is almost double that of the original macroalgal feedstock, measuring between 17.52 and 19.46 MJ kg^{-1}. However, this value is slightly lower compared to the HHV of biochar obtained from *U. lactuca* (19.94−21.61 MJ kg^{-1})[20] and *S. plagiophyllum* (23.12−25.89 MJ kg^{-1}),[13] both types of green and brown macroalgae, respectively.

When assessing the qualities of biomass for energy applications, it is essential to consider factors beyond the HHV, such as the atomic ratios of O/C and H/C. It is essential to note that the chemical energies of bonds involving carbon and oxygen (C−O) and carbon and hydrogen (C−H) are lower than those of carbon−carbon (C−C) bonds.[45] Consequently, biomass characterized by lower atomic ratios of 0:1 and 0:2 generally possesses a higher content of energy. The alterations in atomic ratios of O/C and H/C observed in the Van Krevelen diagram (Figure 6), depicting the pyrolysis of *K. cottonii*, indicate the prevalence of decarboxylation and dehydration reactions during the process. The resulting biochar exhibits reduced atomic ratios of O/C and H/C in comparison to the macroalgal biomass, confirming the presence of these reactions. Specifically, the atomic ratios of H/C and O/C decrease significantly from 2.11 and 1.35, respectively, for the feedstock to 0.98 and 0.91 at 400 °C, 0.94 and 0.87 at 500 °C, and 0.74 and 0.87 at 600 °C for the biochar. According to Zhou et al.,[33] enhancement of biochar's energy content can be attributed to the reduction in energy of

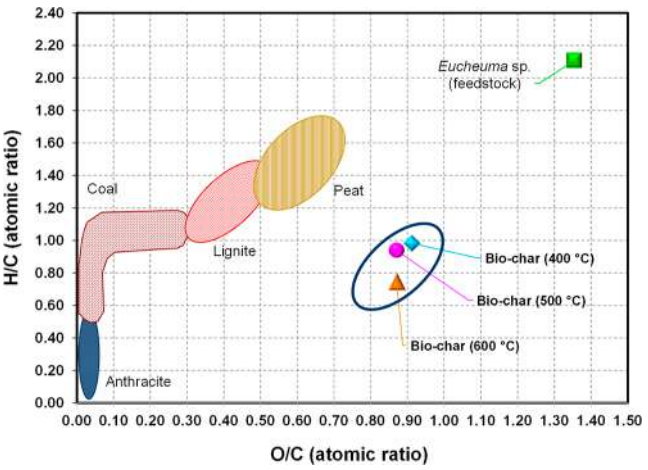

Figure 6. Van Krevelen diagram of the biochar derived from rejected *K. cottonii* pyrolysis.

https://doi.org/10.1021/acsomega.4c00678
ACS Omega 2024, 9, 16665−16675

C−O and C−H bonds, as well as the increased energy of C−C bonds. As a result, the HHV of the biochar derived from the slow pyrolysis of *K. cottonii* surpasses that of the initial feedstock.

3.4.2. Functional Group Analysis. FTIR analysis was employed to analyze the functional groups present in biochar derived from the slow pyrolysis of *K. cottonii*. Figure 7 displays

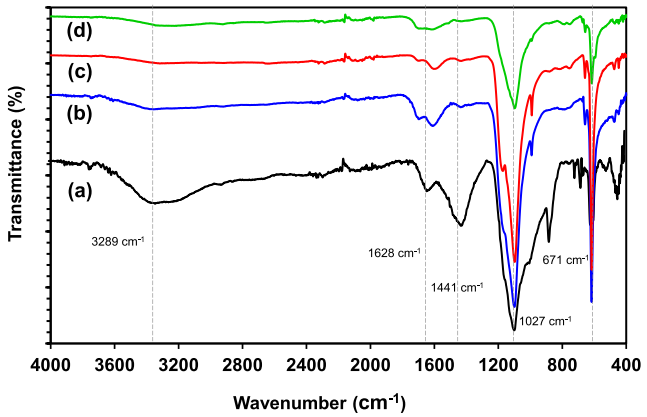

Figure 7. FTIR spectra of (a) rejected *K. cottonii*, (b) biochar at 400 °C, (c) biochar at 500 °C, and (d) biochar at 600 °C.

the FTIR spectra of the biochar as well as the initial feedstock for comparison purposes. Observations indicate that the broad peak at 3280 cm^{-1}, representing the stretching vibration of the O−H bonds, was present in the *K. cottonii* feedstock but disappeared in the FTIR spectra of the resulting biochar. This disappearance confirms the dehydration process that occurs during pyrolysis. Additionally, small peaks at 1628 and 1584 cm^{-1}, indicating secondary amine bends and the presence of nitrogen, were observed in the FTIR spectra. The peak at 1584 cm^{-1} disappeared when the temperature exceeded 500 °C. This might be because the amino acids present in the algal feedstock undergo deamination reactions.

The FTIR analysis revealed prominent peaks at 1027 cm^{-1}, indicating the existence of aromatic compounds in the biochar. These peaks correspond to the stretching vibrations of the C−H functional group in the aromatic. Additionally, several peaks at 671 cm^{-1} were detected, associated with the presence of polycyclic aromatic hydrocarbons that can form during the pyrolysis of algal feedstock.[1] This observation in the FTIR spectra aligns with the findings of a prior study by Iaccarino et al., who reported similar peaks associated with aromatic structures at 874 cm^{-1} in the biochar derived from *S. bigelovii* pyrolysis.[1] In general, the FTIR spectra of biochar derived from *K. cottonii* via slow pyrolysis reveal the presence of aromatic compounds, likely stemming from the prevalent occurrence of polycyclic aromatic compounds in the biochar.[32]

3.4.3. Surface Properties. This section explores the surface morphology, pore size distribution, and surface area of biochar derived from *K. cottonii* pyrolysis. SEM was utilized to examine the surface morphology of the initial biomass and its corresponding biochar. Figure 8 presents side-by-side SEM images depicting the macroalgal biomass and its biochar derived from the slow pyrolysis of *K. cottonii*. It is evident that the macroalgal biomass and biochar exhibit distinct morphological characteristics. Interestingly, the biochar exhibits a higher level of porosity compared to that of the macroalgal feedstock. The pyrolysis process causes the spherical shape of the raw *K. cottonii* to crack, resulting in the formation of small, porous particles with rough surfaces. The morphology of the biochar exhibits an increased presence of void spaces and a higher level of porosity on its surface, suggesting that the resulting biochar has a larger surface area compared to that of the initial waste material. This enhancement in porosity is a result of thermal degradation, causing the removal of volatile components from the initial algal waste and, consequently, altering its structural framework.

The BET analysis image presented in Figure 9 depicts the properties of the biochar produced from *K. cottonii*. The observed isotherms closely match the typical type IV isotherm profile, suggesting a prominent mesoporous structure within

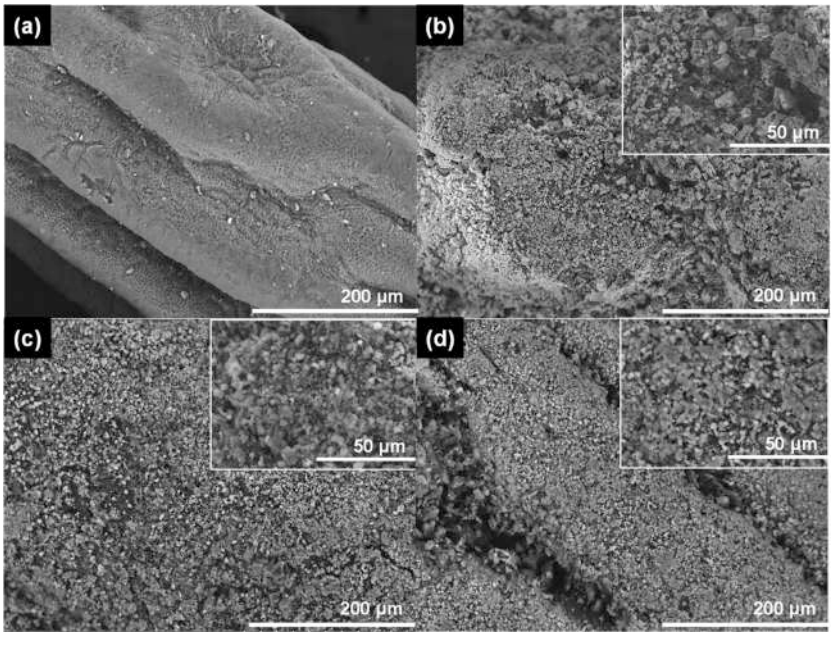

Figure 8. SEM images of (a) rejected *K. cottonii*, (b) biochar at 400 °C, (c) biochar at 500 °C, and (d) biochar at 600 °C.

https://doi.org/10.1021/acsomega.4c00678
ACS Omega 2024, 9, 16665−16675

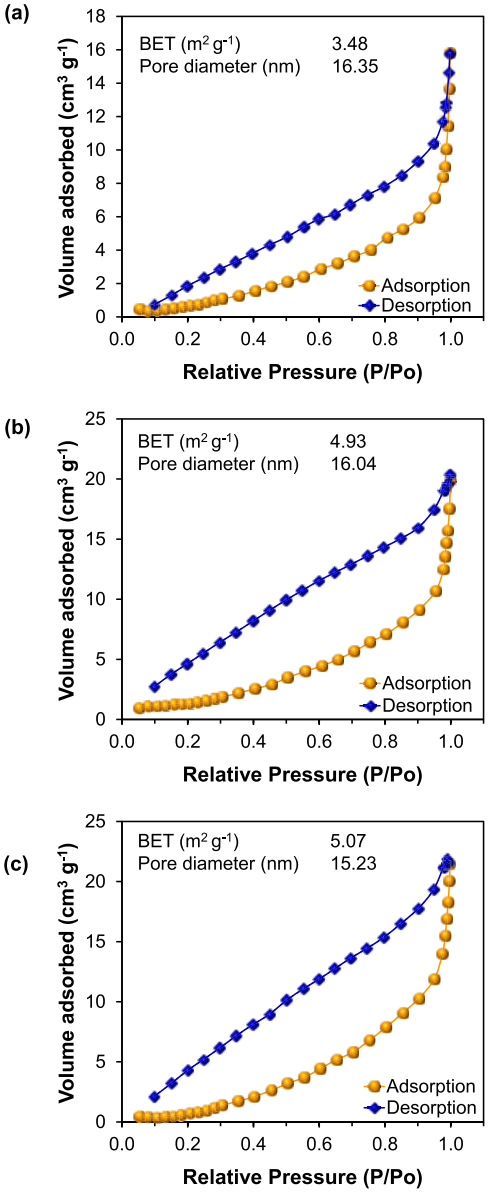

Figure 9. BET analysis image of biochar derived from *K. cottonii* pyrolysis at (b) 400, (c) 500, and (d) 600 °C.

the biochar. Table 3 presents a comparative analysis of the pore sizes in biochar produced at varying temperatures. There

Table 3. BET Surface Area and Pore Characteristics in Macroalgal Biochar

sample	BET surface area [$m^2 g^{-1}$]	total pore volume [$cm^3 g^{-1}$]	mean pore diameter [nm]
biochar (400 °C)	3.48	0.0041	16.35
biochar (500 °C)	4.93	0.0056	16.04
biochar (600 °C)	5.07	0.0062	15.23

was a modest increase in the biochar's surface area from 3.48 to 5.07 $m^2 g^{-1}$ as the pyrolysis temperature increased. These results align with prior research by Iaccarino et al.,[1] which reported that the surface area of biochar obtained from pretreated samples varied between 5.33 and 7.94 $m^2 g^{-1}$. The development of the surface area and porosity in biochar can be ascribed to the swift volatilization of compounds at elevated temperatures, which leads to the creation of an open, porous framework. Nonetheless, it is pertinent to point out that the surface area of biochar obtained from macroalgae is generally less than that of biochar derived from terrestrial plants. As an example, Muzyka et al.[46] noted a considerably higher surface area of 400 $m^2 g^{-1}$ for biochar derived from wheat straw pyrolysis at 700 °C with a heating rate of 20 °C per minute. The difference in surface area might stem from the greater lignin content in land-based plants in contrast to that of macroalgae.[16] Another possible factor contributing to the lower surface area of macroalgae-derived biochar is the high salt content in macroalgae, which may lead to pore clogging.[1]

4. CONCLUSIONS

This research delves into the untapped potential of rejected *K. cottonii* biomass through the application of slow pyrolysis, offering a sustainable and alternative pathway for the production of bio-oil and biochar. The temperature and duration of pyrolysis reactions significantly influence the composition of the resulting products. Bio-oil yield exhibits an increasing trend up to 500 °C, after which it begins to decrease when the temperature is further elevated. Simultaneously, gaseous product yields rise, while biochar yields decrease with an increasing temperature. Bio-oil and biochar yields as high as 28.51 and 52.59%, respectively, are achieved at 500 °C for 50 min. Analysis of bio-oils reveals a diverse composition comprising substantial amounts of furan derivatives, aliphatic hydrocarbons, and carboxylic acids. The biochar produced through slow pyrolysis exhibits calorific values within a noteworthy range (17.52−19.46 MJ kg^{-1}). Results from the ultimate analysis suggest that the atomic ratios of H/C and O/C in biochar are reduced compared with those in the initial biomass, confirming dehydration and decarboxylation reactions during pyrolysis. In summary, the slow pyrolysis of rejected *K. cottonii* emerges as a promising avenue for valorizing marine biomass. This process not only offers a sustainable waste management solution but also provides valuable resources for bioenergy and diverse industrial applications. The findings establish a foundational understanding for further exploration and application of slow pyrolysis as an environmentally friendly approach to the utilization of macroalgal biomass.

■ ASSOCIATED CONTENT

Supporting Information

The Supporting Information is available free of charge at https://pubs.acs.org/doi/10.1021/acsomega.4c00678.

Chemical composition identified in bio-oil by GC/MS from pyrolysis of *K. cottonii* and typical GC/MS chromatogram of rejected *K. cottonii* bio-oil at operating pyrolysis temperatures of 400, 500, and 600 °C (PDF)

■ AUTHOR INFORMATION

Corresponding Author

Obie Farobie − *Department of Mechanical and Biosystem Engineering, IPB University, Bogor, West Java 16680, Indonesia;* orcid.org/0000-0002-6159-635X; Phone: +62-812-898-11-381; Email: obiefarobie@apps.ipb.ac.id

https://doi.org/10.1021/acsomega.4c00678
ACS Omega 2024, 9, 16665−16675

Authors

Apip Amrullah − *Department of Mechanical Engineering, Lambung Mangkurat University, Banjarmasin, South of Kalimantan 70123, Indonesia*

Novi Syaftika − *Research Center for Industrial Process and Manufacturing Technology, National Research and Innovation Agency Republic of Indonesia, Selatan, Banten 10340, Indonesia*

Asep Bayu − *Research Center for Vaccine and Drugs, National Research and Innovation Agency Republic of Indonesia, Bogor, West Java 16911, Indonesia;* orcid.org/0000-0002-5693-0501

Edy Hartulistiyoso − *Department of Mechanical and Biosystem Engineering, IPB University, Bogor, West Java 16680, Indonesia*

Widya Fatriasari − *Research Center for Biomass and Bioproducts, National Research and Innovation Agency Republic of Indonesia, Bogor, West Java 16911, Indonesia*

Asep Bayu Dani Nandiyanto − *Universitas Pendidikan Indonesia, Bandung, West Java 40154, Indonesia*

Complete contact information is available at: https://pubs.acs.org/10.1021/acsomega.4c00678

Notes

The authors declare no competing financial interest.

■ ACKNOWLEDGMENTS

The authors would like to express their immense gratitude for the support received from the Indonesian Endowment Fund for Education (LPDP) and the Indonesian Science Fund (DIPI) through the International Collaboration RISPRO Funding Program "RISPRO KI" (grant no. RISPRO/KI/B1/KOM/12/11684/1/2020).

■ REFERENCES

(1) Iaccarino, A.; Gautam, R.; Sarathy, S. M. Bio-Oil and Biochar Production from Halophyte Biomass: Effects of Pre-Treatment and Temperature on Salicornia Bigelovii Pyrolysis. *Sustain. Energy Fuels* **2021**, *5* (8), 2234−2248.

(2) Barontini, F.; Biagini, E.; Tognotti, L. Influence of Torrefaction on Biomass Devolatilization. *ACS Omega* **2021**, *6* (31), 20264−20278.

(3) Wang, Y.; Liu, Y.; Wang, W.; Liu, L.; Hu, C. Torrefaction at 200 °C of *Pubescens* Pretreated with $AlCl_3$ Aqueous Solution at Room Temperature. *ACS Omega* **2020**, *5* (42), 27709−27722.

(4) Samanmulya, T.; Farobie, O.; Matsumura, Y. Gasification Characteristics of Aminobutyric Acid and Serine as Model Compounds of Proteins under Supercritical Water Conditions. *J. Jpn. Pet. Inst.* **2017**, *60* (1), 34−40.

(5) Gao, Y.; Wang, M.; Raheem, A.; Wang, F.; Wei, J.; Xu, D.; Song, X.; Bao, W.; Huang, A.; Zhang, S.; Zhang, H. Syngas Production from Biomass Gasification: Influences of Feedstock Properties, Reactor Type, and Reaction Parameters. *ACS Omega* **2023**, *8* (35), 31620−31631.

(6) Bhattarai, A.; Kemp, A.; Jahromi, H.; Kafle, S.; Adhikari, S. Thermochemical Characterization and Kinetics of Biomass, Municipal Plastic Waste, and Coal Blends and their Potential for Energy Generation via Gasification. *ACS Omega* **2023**, *8* (48), 45985−46001.

(7) Amrullah, A.; Farobie, O.; Widyanto, R. Pyrolysis of Purun Tikus (Eleocharis Dulcis): Product Distributions and Reaction Kinetics. *Bioresour. Technol. Rep.* **2021**, *13*, 100642.

(8) Tahir, M. H.; Irfan, R. M.; Hussain, M. B.; Alhumade, H.; Al-Turki, Y.; Cheng, X.; Karim, A.; Ibrahim, M.; Rathore, H. A. Catalytic Fast Pyrolysis of Soybean Straw Biomass for Glycolaldehyde-Rich Bio-Oil Production and Subsequent Extraction. *ACS Omega* **2021**, *6* (49), 33694−33700.

(9) Maneechakr, P.; Karnjanakom, S. Improving the Bio-Oil Quality via Effective Pyrolysis/Deoxygenation of Palm Kernel Cake over a Metal (Cu, Ni, or Fe)-Doped Carbon Catalyst. *ACS Omega* **2021**, *6* (30), 20006−20014.

(10) Dhyani, V.; Bhaskar, T. A Comprehensive Review on the Pyrolysis of Lignocellulosic Biomass. *Renewable Energy* **2018**, *129*, 695−716.

(11) Anex, R. P.; Aden, A.; Kazi, F. K.; Fortman, J.; Swanson, R. M.; Wright, M. M.; Satrio, J. A.; Brown, R. C.; Daugaard, D. E.; Platon, A.; Kothandaraman, G.; Hsu, D. D.; Dutta, A. Techno-Economic Comparison of Biomass-to-Transportation Fuels via Pyrolysis, Gasification, and Biochemical Pathways. *Fuel* **2010**, *89* (Suppl. 1), S29−S35.

(12) Balagurumurthy, B.; Singh, R.; Bhaskar, T. *Catalysts for Thermochemical Conversion of Biomass*; Elsevier B.V., 2015..

(13) Farobie, O.; Amrullah, A.; Bayu, A.; Syaftika, N.; Anis, L. A.; Hartulistiyoso, E. In-Depth Study of Bio-Oil and Biochar Production from Macroalgae Sargassum Sp. via Slow Pyrolysis. *RSC Adv.* **2022**, *12* (16), 9567−9578.

(14) Sakhiya, A. K.; Anand, A.; Aier, I.; Vijay, V. K.; Kaushal, P. Suitability of Rice Straw for Biochar Production through Slow Pyrolysis: Product Characterization and Thermodynamic Analysis. *Bioresour. Technol. Rep.* **2021**, *15*, 100818.

(15) Okonkwo, C. A.; Menkiti, M. C.; Obiora-Okafo, I. A.; Ezenwa, O. N. Controlled Pyrolysis of Sugarcane Bagasse Enhanced Mesoporous Carbon for Improving Capacitance of Supercapacitor Electrode. *Biomass Bioenergy* **2021**, *146*, 105996.

(16) Farobie, O.; Matsumura, Y.; Syaftika, N.; Amrullah, A.; Hartulistiyoso, E.; Bayu, A.; Moheimani, N. R.; Karnjanakom, S.; Saefurahman, G. Recent Advancement on Hydrogen Production from Macroalgae via Supercritical Water Gasification. *Bioresour. Technol. Rep.* **2021**, *16*, 100844.

(17) Ly, H. V.; Kim, S. S.; Woo, H. C.; Choi, J. H.; Suh, D. J.; Kim, J. Fast Pyrolysis of Macroalga Saccharina Japonica in a Bubbling Fluidized-Bed Reactor for Bio-Oil Production. *Energy* **2015**, *93*, 1436−1446.

(18) Farghali, M.; Ap, Y.; Mohamed, I. M. A.; Iwasaki, M.; Tangtaweewipat, S.; Ihara, I.; Sakai, R.; Umetsu, K. Thermophilic Anaerobic Digestion of Sargassum Fulvellum Macroalgae: Biomass Valorization and Biogas Optimization under Different Pre-Treatment Conditions. *J. Environ. Chem. Eng.* **2021**, *9* (6), 106405.

(19) Jumaidin, R.; Sapuan, S. M.; Jawaid, M.; Ishak, M. R.; Sahari, J. Characteristics of Eucheuma Cottonii Waste from East Malaysia: Physical, Thermal and Chemical Composition. *Eur. J. Phycol.* **2017**, *52* (2), 200−207.

(20) Amrullah, A.; Farobie, O.; Bayu, A.; Syaftika, N.; Hartulistiyoso, E.; Moheimani, N. R.; Karnjanakom, S.; Matsumura, Y. Slow Pyrolysis of Ulva Lactuca (Chlorophyta) for Sustainable Production of Bio-Oil and Biochar. *Sustainability* **2022**, *14* (6), 3233.

(21) Saeed, A. A. H.; Harun, N. Y.; Sufian, S.; Siyal, A. A.; Zulfiqar, M.; Bilad, M. R.; Vagananthan, A.; Al-Fakih, A.; Ghaleb, A. A. S.; Almahbashi, N. Eucheuma Cottonii Seaweed-Based Biochar for Adsorption of Methylene Blue Dye. *Sustainability* **2020**, *12* (24), 10318.

(22) Saldarriaga-Hernandez, S.; Melchor-Martínez, E. M.; Carrillo-Nieves, D.; Parra-Saldívar, R.; Iqbal, H. M. N. Seasonal Characterization and Quantification of Biomolecules from Sargassum Collected from Mexican Caribbean Coast—A Preliminary Study as a Step Forward to Blue Economy. *J. Environ. Manage.* **2021**, *298*, 113507.

(23) Mohamed Noor, N.; Shariff, A.; Abdullah, N.; Mohamad Aziz, N. S. Temperature Effect on Biochar Properties from Slow Pyrolysis of Coconut Flesh Waste. *Malays. J. Fundam. Appl. Sci.* **2019**, *15* (2), 153−158.

(24) Kaewpanha, M.; Guan, G.; Hao, X.; Wang, Z.; Kasai, Y.; Kusakabe, K.; Abudula, A. Steam Co-Gasification of Brown Seaweed and Land-Based Biomass. *Fuel Process. Technol.* **2014**, *120*, 106−112.

(25) Li, B.; Li, C.; Li, D.; Jiang, Y.; Zhang, L.; Zhang, S.; Wang, Y.; Hu, S.; Xiang, J.; Hu, X. Cross-Interaction of Volatiles in Co-Pyrolysis of Spinach and Noodles and their Impacts on Properties of Pyrolytic Products and Pyrolysis Kinetics. *J. Environ. Chem. Eng.* **2023**, *11* (3), 110276.
(26) Bayu, A.; Warsito, M. F.; Putra, M. Y.; Karnjanakom, S.; Guan, G. Macroalgae-Derived Rare Sugars: Applications and Catalytic Synthesis. *Carbon Resour. Convers.* **2021**, *4*, 150−163.
(27) Wang, S.; Xia, Z.; Wang, Q.; He, Z.; Li, H. Mechanism Research on the Pyrolysis of Seaweed Polysaccharides by Py-GC/MS and Subsequent Density Functional Theory Studies. *J. Anal. Appl. Pyrolysis* **2017**, *126*, 118−131.
(28) Abirami, R. G.; Kowsalya, S. Nutrient and Nutraceutical Potentials of Seaweed Biomass Ulva Lactuca and Kappaphycus Alvarezii. *Agric. Sci. Technol.* **2011**, *5* (1), 1−7.
(29) Nallasivam, J.; Francis Prashanth, P.; Harisankar, S.; Nori, S.; Suryanarayan, S.; Chakravarthy, S. R.; Vinu, R. Valorization of Red Macroalgae Biomass via Hydrothermal Liquefaction Using Homogeneous Catalysts. *Bioresour. Technol.* **2022**, *346*, 126515.
(30) Øverland, M.; Mydland, L. T.; Skrede, A. Marine Macroalgae as Sources of Protein and Bioactive Compounds in Feed for Monogastric Animals. *J. Sci. Food Agric.* **2019**, *99* (1), 13−24.
(31) Sun, J.; Norouzi, O.; Mašek, O. A State-of-the-Art Review on Algae Pyrolysis for Bioenergy and Biochar Production. *Bioresour. Technol.* **2022**, *346*, 126258.
(32) Aboulkas, A.; Hammani, H.; El Achaby, M.; Bilal, E.; Barakat, A.; El harfi, K. Valorization of Algal Waste via Pyrolysis in a Fixed-Bed Reactor: Production and Characterization of Bio-Oil and Bio-Char. *Bioresour. Technol.* **2017**, *243*, 400−408.
(33) Zhou, S.; Liang, H.; Han, L.; Huang, G.; Yang, Z. The Influence of Manure Feedstock, Slow Pyrolysis, and Hydrothermal Temperature on Manure Thermochemical and Combustion Properties. *Waste Manag.* **2019**, *88*, 85−95.
(34) Gautam, R.; Shyam, S.; Reddy, B. R.; Govindaraju, K.; Vinu, R. Microwave-Assisted Pyrolysis and Analytical Fast Pyrolysis of Macroalgae: Product Analysis and Effect of Heating Mechanism. *Sustain. Energy Fuels* **2019**, 3 (11), 3009−3020.
(35) Vinu, R.; Broadbelt, L. J. A Mechanistic Model of Fast Pyrolysis of Glucose-Based Carbohydrates to Predict Bio-Oil Composition. *Energy Environ. Sci.* **2012**, *5* (12), 9808−9826.
(36) Zhou, X.; Li, W.; Mabon, R.; Broadbelt, L. J. A Mechanistic Model of Fast Pyrolysis of Hemicellulose. *Energy Environ. Sci.* **2018**, *11* (5), 1240−1260.
(37) Persson, H.; Yang, W. Catalytic Pyrolysis of Demineralized Lignocellulosic Biomass. *Fuel* **2019**, *252*, 200−209.
(38) Zhang, L.; Yang, Z.; Li, S.; Wang, X.; Lin, R. Comparative Study on the Two-Step Pyrolysis of Different Lignocellulosic Biomass: Effects of Components. *J. Anal. Appl. Pyrolysis* **2020**, *152*, 104966.
(39) Zong, P.; Jiang, Y.; Tian, Y.; Li, J.; Yuan, M.; Ji, Y.; Chen, M.; Li, D.; Qiao, Y. Pyrolysis Behavior and Product Distributions of Biomass Six Group Components: Starch, Cellulose, Hemicellulose, Lignin, Protein and Oil. *Energy Convers. Manag.* **2020**, *216*, 112777.
(40) Su, Y.; Liu, L.; Zhang, S.; Xu, D.; Du, H.; Cheng, Y.; Wang, Z.; Xiong, Y. A Green Route for Pyrolysis Poly-Generation of Typical High Ash Biomass, Rice Husk: Effects on Simultaneous Production of Carbonic Oxide-Rich Syngas, Phenol-Abundant Bio-Oil, High-Adsorption Porous Carbon and Amorphous Silicon Dioxide. *Bioresour. Technol.* **2020**, *295*, 122243.
(41) Zhang, Z. B.; Lu, Q.; Ye, X. N.; Li, W. T.; Hu, B.; Dong, C. Q. Production of Phenolic-Rich Bio-Oil from Catalytic Fast Pyrolysis of Biomass Using Magnetic Solid Base Catalyst. *Energy Convers. Manag.* **2015**, *106*, 1309−1317.
(42) Wang, X.; Tang, X.; Yang, X. Pyrolysis Mechanism of Microalgae Nannochloropsis Sp. Based on Model Compounds and their Interaction. *Energy Convers. Manag.* **2017**, *140*, 203−210.
(43) Zhao, C.; Jiang, E.; Chen, A. Volatile Production from Pyrolysis of Cellulose, Hemicellulose and Lignin. *J. Energy Inst.* **2017**, *90* (6), 902−913.
(44) Reyes, L.; Abdelouahed, L.; Mohabeer, C.; Buvat, J. C.; Taouk, B. Energetic and Exergetic Study of the Pyrolysis of Lignocellulosic Biomasses, Cellulose, Hemicellulose and Lignin. *Energy Convers. Manag.* **2021**, *244*, 114459.
(45) Zhao, P.; Shen, Y.; Ge, S.; Chen, Z.; Yoshikawa, K. Clean Solid Biofuel Production from High Moisture Content Waste Biomass Employing Hydrothermal Treatment. *Appl. Energy* **2014**, *131*, 345−367.
(46) Muzyka, R.; Misztal, E.; Hrabak, J.; Banks, S. W.; Sajdak, M. Various Biomass Pyrolysis Conditions Influence the Porosity and Pore Size Distribution of Biochar. *Energy* **2023**, *263*, 126128.

https://doi.org/10.1021/acsomega.4c00678
ACS Omega 2024, 9, 16665−16675